Article

Water-Soluble Cruciforms: Response to Protons and Selected Metal Ions

Juan Tolosa, Anthony J. Zucchero, and Uwe H. F. Bunz

J. Am. Chem. Soc., **2008**, 130 (20), 6498-6506 • DOI: 10.1021/ja800232f • Publication Date (Web): 24 April 2008

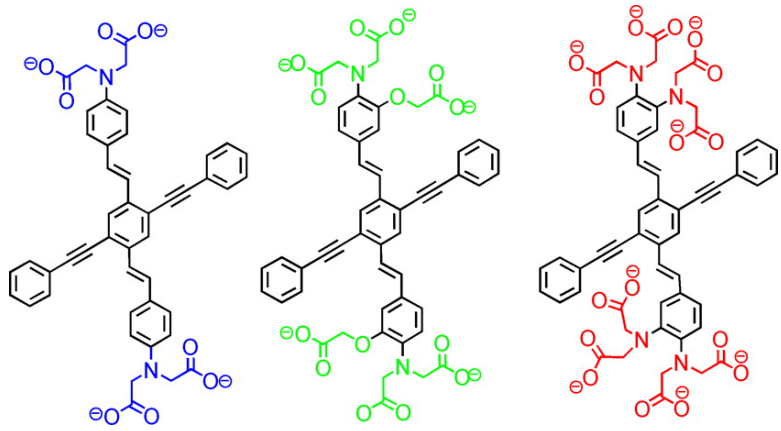

More About This Article

Additional resources and features associated with this article are available within the HTML version:

- Supporting Information
- Access to high resolution figures
- Links to articles and content related to this article
- Copyright permission to reproduce figures and/or text from this article

View the Full Text HTML

J|A|C|S
ARTICLES

Published on Web 04/24/2008

Water-Soluble Cruciforms: Response to Protons and Selected Metal Ions

Juan Tolosa, Anthony J. Zucchero, and Uwe H. F. Bunz*

School of Chemistry and Biochemistry, Georgia Institute of Technology, 901 Atlantic Drive, Atlanta, Georgia 30332

Received January 10, 2008; E-mail: uwe.bunz@chemistry.gatech.edu

Abstract: The syntheses of three water-soluble cruciform fluorophores (XF) carrying aniline-*N,N*-bisacetic acid, 2-hydroxyaniline-*N,N,O*-trisacetic acid, and 1,2-phenylenediamine-*N,N,N′,N′*-tetrakisacetic acid are reported. The XF skeleton was synthesized by a Horner reaction to assemble the distyrylbenzene unit followed by a Sonogashira coupling to attach the phenyleneethynylene modules. The photophysics of both the sodium salts and the ethyl esters of the three carboxylated 1,4-bis(aminostyryl)-2,5-bis(phenylethynyl)-benzenes were investigated in chloroform and in aqueous buffered solution at a pH of 7.0 and compared to that of 1,4-bis(dibutylaminostyryl)-2,5-bis(phenylethynyl)benzene (BDB). The attachment of the carboxylate units to the aniline nitrogens influenced the photophysics and the sensory responses of the XFs, as the combined effect of steric bulk and charge repulsion led to a blue-shifted absorption when compared to that of BDB. While the fluorescence of the water-soluble XFs is sensitive toward metal cations, the mode of sensing action is different from that of BDB, where direct complexation to the aniline nitrogen lowers the energy of the HOMO (but not of the LUMO), leading to a blue-shifted emission. In the case of the 2-hydroxyaniline-*N,N,O*-trisacetic acid and 1,2-phenylenediamine-*N,N,N′,N′*-tetrakisacetic acid-functionalized XFs, interaction with metal cations in aqueous buffered solution is guided by a breakup of excimers that form in water at XF concentrations as low as 50 μmol·L^{-1}.

Introduction

We describe herein the synthesis, photophysics, and metalloresponsive properties of three consanguine, ionic, water-soluble cruciforms (XF) **5**–**7**. The XFs **5**–**7**, even though they share a common chromophore with **8**, display surprisingly different photophysical properties from each other and from the model XF **8**, carrying dibutylamino substituents.

Metalloresponsive fluorophores[1,2] and chromophores are of scientific and practical interest to detect metal cations in compartmentalized biological systems such as eukaryotic cells.[3–7] Metal cations with prominent biological functions in cells are iron, copper, zinc, magnesium, and calcium but also vanadium and manganese.[8,9] A second area of interest for metalloresponsive fluorophores is the detection of environmentally harmful metals such as lead and mercury.[10–13] Both of these divergent fields may use similar design principles for their metallophores, yet there are marked differences. For environmental sensing, a successful metalloresponsive fluorophore would need high binding constants to ensure detection limits in the parts per billion range. It is not clear if metalloresponsive fluorophores

(1) Henary, M. M.; Wu, Y. G.; Fahrni, C. J. *Chem.—Eur. J.* **2004**, *10*, 3015–3025.
(2) (a) Wang, B.; Wasielewski, M. R. *J. Am. Chem. Soc.* **1997**, *119*, 12–21. (b) Bangcuyo, C. G.; Rampey-Vaughn, M. E.; Quan, L. T.; Angel, S. M.; Smith, M. D.; Bunz, U. H. F. *Macromolecules* **2002**, *35*, 1563–1568. (c) Pautzsch, T.; Klemm, E. *Macromolecules* **2002**, *35*, 1569–1575.
(3) Pond, S. J. K.; Tsutsumi, O.; Rumi, M.; Kwon, O.; Zojer, E.; Bredas, J. L.; Marder, S. R.; Perry, J. W. *J. Am. Chem. Soc.* **2004**, *126*, 9291–9306.
(4) Lim, N. C.; Freake, H. C.; Brückner, C. *Chem.—Eur. J.* **2005**, *11*, 38–49.
(5) Pearce, D. A.; Jotterand, N.; Carrico, I. S.; Imperiali, B. *J. Am. Chem. Soc.* **2001**, *123*, 5160–5161.
(6) (a) Burdette, S. C.; Walkup, G. K.; Spingler, B.; Tsien, R. Y.; Lippard, S. J. *J. Am. Chem. Soc.* **2001**, *123*, 7831–7841. (b) Walkup, G. K.; Burdette, S. C.; Lippard, S. J.; Tsien, R. Y. *J. Am. Chem. Soc.* **2000**, *122*, 5644–5645.
(7) (a) Hirano, T.; Kikuchi, K.; Urano, Y.; Higuchi, T.; Nagano, T. *J. Am. Chem. Soc.* **2000**, *122*, 12399–12400. (b) Hirano, T.; Kikuchi, K.; Urano, Y.; Nagano, T. *J. Am. Chem. Soc.* **2002**, *124*, 6555–6562. (c) Komatsu, K.; Kikuchi, K.; Kojima, H.; Urano, Y.; Nagano, T. *J. Am. Chem. Soc.* **2005**, *127*, 10197–10204. (d) Kawabata, E.; Kikuchi, K.; Urano, Y.; Kojima, H.; Odani, A.; Nagano, T. *J. Am. Chem. Soc.* **2005**, *127*, 818–819.
(8) (a) Hofer, A. M.; Machen, T. E. *Proc. Natl. Acad. Sci. U.S.A.* **1993**, *90*, 2598–2602. (b) Sensi, S. L.; Canzoniero, L. M. T.; Yu, S. P.; Ying, H. S.; Koh, J. Y.; Kerchner, G. A.; Choi, D. W. *J. Neurosci.* **1997**, *17*, 9554–9564. (c) Zhao, M. D.; Hollingworth, S.; Baylor, S. M. *Biophys. J.* **1996**, *70*, 896–916. (d) Metten, B.; Smet, M.; Boens, N.; Dehaed, W. *Synthesis* **2005**, 1838–1844.
(9) (a) Zhou, Z.; Fahrni, C. J. *J. Am. Chem. Soc.* **2004**, *126*, 8862–8863. (b) Yang, L. C.; McRae, R.; Henary, M. M.; Patel, R.; Lai, B.; Vogt, S.; Fahrni, C. J. *Proc. Natl. Acad. Sci. U.S.A.* **2005**, *102*, 11179–11184. (c) Cody, J.; Fahrni, C. J. *Tetrahedron* **2004**, *60*, 11099–11107. (d) Corradini, R.; Dossena, A.; Galaverna, G.; Marchelli, R.; Panagia, A.; Sartor, G. *J. Org. Chem.* **1997**, *62*, 6283–6289.
(10) Kim, I.-B.; Dunkhorst, A.; Gilbert, J.; Bunz, U. H. F. *Macromolecules* **2005**, *38*, 4560–4562.
(11) Kim, I.-B.; Erdogan, B.; Wilson, J. N.; Bunz, U. H. F. *Chem.—Eur. J.* **2004**, *10*, 6247–6254.
(12) (a) Chen, C. T.; Huang, W. P. *J. Am. Chem. Soc.* **2002**, *124*, 6246–6247. (b) Aragoni, M. C.; Arca, M.; Demartin, F.; Devillanova, F. A.; Isaia, F.; Garau, A.; Lippolis, V.; Jalali, F.; Papke, U.; Shamsipur, M.; Tei, L.; Yari, A.; Verani, G. *Inorg. Chem.* **2002**, *41*, 6623–6632.
(13) (a) Thomas, S. W.; Joly, G. D.; Guy, D.; Swager, T. M. *Chem. Rev.* **2007**, *107*, 1339–1386. (b) Ono, A.; Togashi, H. *Angew. Chem.* **2004**, *43*, 4300–4302. (c) Kim, Y. H.; Youk, J. S.; Moon, S. Y.; Choe, J. I.; Chang, S. K. *Chem. Lett.* **2004**, *33*, 702–703. (d) Nolan, E. M.; Lippard, S. J. *J. Am. Chem. Soc.* **2003**, *125*, 14270–14271.

10.1021/ja800232f CCC: $40.75

can detect environmental pollutants such as mercury ions at levels that are merely elevated but not (yet) toxic. For fluorophores reporting metal ions in cells, the sensitivity issue is less severe. The *local* concentration of a specific metal cation can be high in cellular compartments presenting pools of free metal ions.[14] An example is that of zinc ions in neuron slices, which are detected by metalloresponsive fluorophores.[4,15]

While metallofluorophores have advanced, their design can still be improved. High quantum yield in water, robust ratiometric response to metals with large changes of wavelengths, and manipulation of absorption and emission wavelengths are only partially solved problems. In addition, some metallofluorophores are not well-soluble in water; cell staining experiments have to be performed by predissolving these fluorophores in DMSO, adding water, and then incubating cells with these dyes. This technique will almost certainly lead to aggregation or nanocrystal formation of the employed fluorophores.[4] Nanocrystals can be endocytized into cell compartments and may persist there, with all accompanying problems for a successful sensing experiment. It is imperative to investigate "design" fluorophores in vitro to understand their photophysical properties before undertaking cell studies.

We have recently reported 1,4-bis(arylethynyl)-2,5-distyrylbenzenes as novel fluorophores.[16] These XFs are synthesized by a Horner reaction followed by a Sonogashira coupling;[17,18] donor–acceptor-substituted XFs feature spatially addressable frontier molecular orbitals.[19–26] Exposure of a dibutylamino-substituted XF, such as **8**, to metal cations results in large hypsochromic shifts in emission that are convincingly explained by stabilization of their HOMO, which is localized on the bis(aminostyryl) axis, through the addition of a positive charge. We investigated XFs of the type **A** (Scheme 1) to understand their photophysics and expand this concept to water-soluble cruciforms **5**–**7** that contain phenylimidobisacetic acid, APTRA,[27] or benzo-EDTA receptor units. We have investigated the pH-dependent photophysical properties of **5**–**7** in absorption and emission and compared them with the photophysical properties of the XF **8**. The results are surprising, as the presence of the anionic charges from the iminobisacetic acid units modulate the photophysical properties of **5**–**7** as compared to **8**. A fundamental change in the interaction paradigm between fluorophores and metal cations is observed when going from **8** to **5**–**7**.

Scheme 1. Interaction of Cruciform Fluorophores with Metal Cations

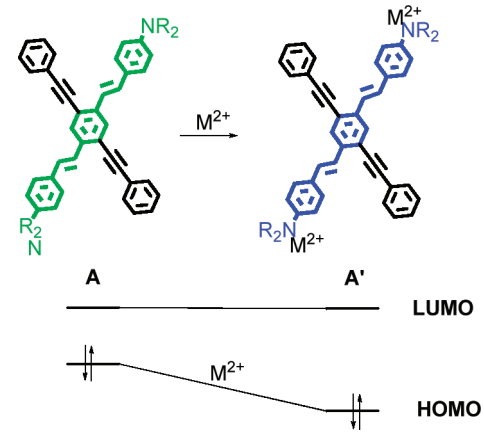

Results and Discussion

Synthesis. The previously reported aldehydes **2**–**4**[28] are obtained from aniline, *ortho*-aminophenol, and *ortho*-phenylenediamine by heating with ethyl bromoacetate in the presence of potassium carbonate in acetone. The esters are subjected to a Vilsmeier formylation, and **2**–**4**[28] are exposed to a mixture of **1**[29] and potassium *tert*-butoxide in THF to give partially saponified distyryldiiodobenzenes (Scheme 2). Due to this partial saponification, the intermediates were not characterized but reacted with phenylacetylene under standard Sonogashira coupling conditions, isolating **5a**−**7a** after careful chromatography; **5a**−**7a** were fully characterized by NMR, IR spectroscopies, and mass spectrometry. The ester groups in **5a**−**7a** were cleaved off under Zempelen conditions to give the sodium salts **5b**−**7b** in 87–95% yield after removal of methanol in vacuo; the yellow powders of **5b**–**7b** dissolve easily in water. For the photophysical

(14) (a) Grynkiewicz, G.; Poenie, M.; Tsien, R. Y. *J. Biol. Chem.* **1985**, *260*, 3440–3450. (b) Minta, A.; Kao, J. P. Y.; Tsien, R. Y. *J. Biol. Chem.* **1989**, *264*, 8171–8178. (c) Zhang, J.; Campbell, R. E.; Ting, A. Y.; Tsien, R. Y. *Nat. Rev. Cell Biol.* **2002**, *3*, 906–918.
(15) (a) Kay, A. R.; Neyton, J.; Paoletti, P. *Neuron* **2006**, *52*, 572–574. (b) Budde, T.; Minta, A.; White, J. A.; Kay, A. R. *Neuroscience* **1997**, *79*, 347–358. (c) Snitsarev, V.; Budde, T.; Stricker, T. P.; Cox, J. M.; Krupa, D. J.; Geng, L.; Kay, A. R. *Biophys. J.* **2001**, *80*, 1538–1546. (d) Suh, S. W.; Jensen, K. B.; Jensen, M. S.; Silva, D. S.; Kesslak, P. J.; Danscher, G.; Frederickson, C. J. *Brain Res.* **2000**, *852*, 274–278.
(16) (a) Wilson, J. N.; Josowicz, M.; Wang, Y. Q.; Bunz, U. H. F. *Chem. Commun.* **2003**, 2962–2963. (b) Wilson, J. N.; Bunz, U. H. F. *J. Am. Chem. Soc.* **2005**, *127*, 4124–412. (c) Gerhardt, W. W.; Zucchero, A. J.; Wilson, J. N.; South, C. R.; Bunz, U. H. F.; Weck, M. *Chem. Commun.* **2006**, 2141–2143. (d) Zucchero, A. J.; Wilson, J. N.; Bunz, U. H. F. *J. Am. Chem. Soc.* **2006**, *128*, 11872–11881.
(17) (a) Horner, L.; Hoffmann, H.; Wippel, H. G.; Klahre, G. *Chem. Ber.* **1959**, *92*, 2499–2505. (b) Meier, H. *Angew. Chem., Int. Ed. Engl.* **1992**, *31*, 1399–1420. (c) Deb, S. K.; Maddux, T. M.; Yu, L. P. *J. Am. Chem. Soc.* **1997**, *119*, 9079–9080. (d) Wang, S. J.; Oldham, W. J.; Hudack, R. A.; Bazan, G. C. *J. Am. Chem. Soc.* **2000**, *122*, 5695–5709. (e) Scherf, U. *Top. Curr. Chem.* **1999**, *201*, 163–222.
(18) (a) Negishi, E.; Anastasia, L. *Chem. Rev.* **2003**, *103*, 1979–2017. (b) Sonogashira, K. *J. Organomet. Chem.* **2002**, *653*, 46–49. (c) Bunz, U. H. F. *Chem. Rev.* **2000**, *100*, 1605–1645.
(19) (a) Marsden, J. A.; Miller, J. J.; Shirtcliff, L. D. *J. Am. Chem. Soc.* **2005**, *127*, 2464–2476. (b) Marsden, J. A.; Haley, M. M. *J. Org. Chem.* **2005**, *70*, 10213–10226. (c) Marsden, J. A.; Miller, J. J.; Haley, M. M. *Angew. Chem., Int. Ed.* **2004**, *43*, 1694–1697.
(20) Klare, J. E.; Tulevski, G. S.; Sugo, K.; de Picciotto, A.; White, K. A.; Nuckolls, C. *J. Am. Chem. Soc.* **2003**, *125*, 6030–6031.
(21) (a) Gobbi, L.; Seiler, P.; Diederich, F. *Angew. Chem., Int. Ed.* **1999**, *38*, 674–678. (b) Diederich, F. *Chem. Commun.* **2001**, 219–227. (c) Tykwinski, R. R.; Gubler, U.; Martin, R. E.; Diederich, F.; Bosshard, C.; Gunter, P. *J. Phys. Chem. B* **1998**, *102*, 4451–4465. (d) Tykwinski, R. R.; Schreiber, M.; Carlon, R. P.; Diederich, F.; Gramlich, V. *Helv. Chim. Acta* **1996**, *79*, 2249–2281. (e) Hilger, A.; Gisselbrecht, J. P.; Tykwinski, R.; Boudon, C.; Schreiber, M.; Martin, R.; Lüthi, H. P.; Gross, M.; Diederich, F. *J. Am. Chem. Soc.* **1997**, *119*, 2069–2078. (f) Mitzel, F.; Boudon, C.; Gisselbrecht, J. P.; Seiler, P.; Gross, M.; Diederich, F. *Helv. Chim. Acta* **2004**, *87*, 1130–1157. (g) Gisselbrecht, J. P.; Moonen, N. N. P.; Boudon, C.; Nielsen, M. B.; Diederich, F.; Gross, M. *Eur. J. Org. Chem.* **2004**, 2959–2972.
(22) Hu, K.; Zhu, P. W.; Yu, Y.; Facchetti, A.; Marks, T. J. *J. Am. Chem. Soc.* **2004**, *126*, 15974–15975.
(23) Niazimbetova, Z. I.; Christian, H. Y.; Bhandari, Y. J.; Beyer, F. L.; Galvin, M. E. *J. Phys. Chem. B* **2004**, *108*, 8673–8681.
(24) Sorensen, J. K.; Vestergaard, M.; Kadziola, A.; Kilsa, K.; Nielsen, M. B. *Org. Lett.* **2006**, *8*, 1173–1176.
(25) Grunder, S.; Huber, R.; Horhoiu, V.; Gonzalez, M. T.; Schonenberger, C.; Calame, M.; Mayor, M. *J. Org. Chem* **2007**, *72*, 8337–8344.
(26) Tolosa, J.; Diez-Barra, E.; Sanchez-Verdu, P.; Rodriguez-Lopez, J. *Tetrahedron Lett.* **2006**, *47*, 4647–4651.
(27) London, R. E. *Annu. Rev. Physiol.* **1991**, *53*, 241–258.
(28) (a) Wang, J.; Quian, X. *Org. Lett.* **2006**, *8*, 3721–3724. (b) Wang, J.; Quian, X.; Cui, J. *J. Org. Chem.* **2006**, *71*, 4308–4311.
(29) Wilson, J. N.; Windscheif, P. M.; Evans, U.; Myrick, M. L.; Bunz, U. H. F. *Macromolecules* **2002**, *35*, 8681–8683.

Scheme 2. Synthesis of Cruciforms **5–7** by a Combination of Horner and Sonogashira Methods

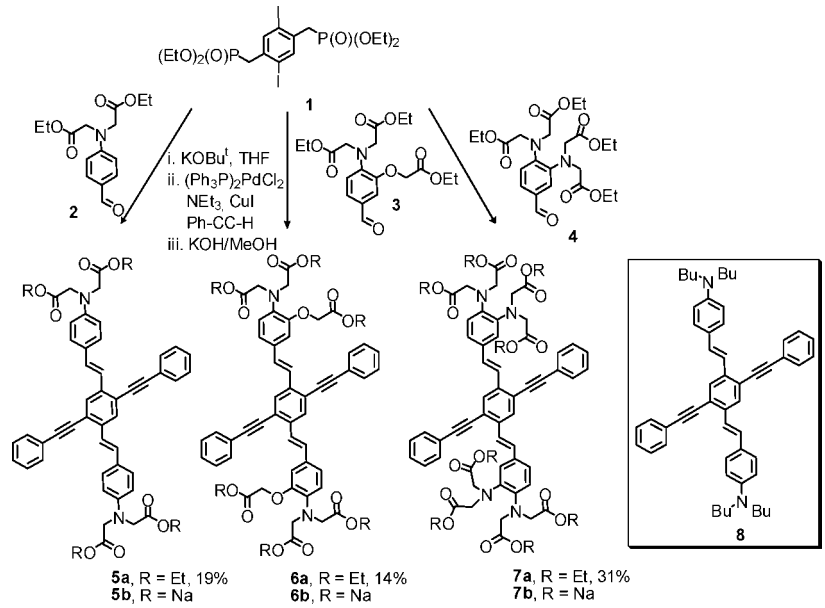

investigations, **5b–7b** were taken up in aqueous phosphate buffer (100 mmol) and titrated to a pH of 7.0. The model compound **8** was synthesized according to refs 16a, d.

Spectroscopic Properties of the Cruciforms 5a−7a and 8 in Dichloromethane. Figure 1 and Table 1 show the absorption and emission spectra of **5a–7a** and **8** in dichloromethane before and after the addition of trifluoroacetic acid. We investigated the influence of the acetic acid groups on the photophysics of the XFs without the complications arising from ionic charges and working in water, facilitating comparison with the model XF **8**: The attachment of the ester groups shifts the absorption spectra of **5a−7a** to the blue when compared to the absorption spectrum of **8**. The effect is strongest in **7a**, where the distinct low energy band visible in **8** at 440 nm is reduced in **7a** to a shoulder at 394 nm. Addition of triethylamine does not appreciably change the absorption spectrum of **7a**, ruling out ground-state protonation as a factor for the loss of the low energy band. In **5a** and **6a**, the low energy feature is blue-shifted when compared to the absorption of **8**. The emission spectrum of **5a** (486 nm) is similar to that of **8**, while that of **6a** is slightly *red*-shifted to 506 nm. Under neutral conditions, the emission spectrum of **7a** is *blue*-shifted to 438 nm and shows a distinct vibronic shoulder. Upon addition of triethylamine, the spectra of **5a**, **6a**, **7a**, and **8** do not change.

Upon addition of acid, **8** shows the well-documented blue shift in absorption and emission.[16] This shift is due to a stabilization of the HOMO (Scheme 1) effected by the protonation of the two dibutylamino groups. The LUMO energy is not affected by the protonation. The same effects as for **8** are observed for **5a**, **6a** and **7a** upon protonation (Figure 1). Disappearance of the low energy transition is coupled with a blue shift in emission. In the case of **7a**, the absorption spectra do not change much upon addition of either acid or base.

The electron-withdrawing acetic acid groups attached to the aniline nitrogen(s) exert a moderate I-effect on the overall distyrylbenzene subunit in **5–7** and should stabilize their HOMO energy. The general blue shift in emission of **5a−7a**, with respect to the emission of **8**, is difficult to explain. It is significant in **5a** but small in **6a**. This shift might be due to the destabilization of the excited state of **6a** by the *meta*-positioned ether group. Upon addition of amine, neither the absorption nor the emission spectra of **5a** or **6a** change, being practically superimposable (Figure 1). Upon addition of trifluoroacetic acid, **8** displays a 124 nm blue shift in absorption under disappearance of the charge transfer band (CT band) and a 94 nm blue shift in emission. In **5a** and **6a**, we see qualitatively similar behavior in absorption, that is, a loss of the CT band and a blue shift in emission, which however is less distinct in **5a** and **6a** than it is in **8**. Again, we presume that particularly in **6a** the excited state of the protonated species is stabilized. In the case of **7a**, we see only the slightest change in absorption upon addition of acid or triethylamine, but in emission, we observe a shift from 503 to 442 nm when going from an amine-added solution to one to which trifluoroacetic acid has been added.

The lack of change in the absorption spectrum combined with a significant blue shift in emission upon protonation in **7a** suggests excited state planarization as a possible explanation;[30] **7a** carries two amine groups per styryl unit. Their high steric congestion forces them into a perpendicular (with respect to the plane of the aromatic system) orientation and deconjugates the free electron pair. Upon going into the first excited state, quinoidal resonance structures will show an increased contribution (Figure 2) and force the *para*-positioned amine (*para* with respect to the central benzene ring) into planarity. Different quinoidal resonance structures are possible, and a representative one is shown in Figure 2. The secondary phenyleneethynylene arm is a convenient acceptor for the negative charge generated when drawing a closed-shell quinoidal resonance structure. The exact electron distribution in the excited state of **7a** is difficult to determine, but this simple resonance argument explains the experimental data.

Spectroscopic Properties of the Cruciforms 5b–7b in Water and 8 in Dichloromethane. In Figure 3, the absorption and emission spectra of **5b−7b** in 100 mmol phosphate buffer are displayed. Overlaid are the absorption and emission spectra of **8** in dichloromethane. The absorption spectra of **5b** and **6b** in

(30) (a) Sluch, M. I.; Godt, A.; Bunz, U. H. F.; Berg, M. A. *J. Am. Chem. Soc.* **2001**, *123*, 6447–6448. (b) Liu, L. T.; Yaron, D.; Berg, M. A. *J. Phys. Chem. C* **2007**, *111*, 5770–5782.

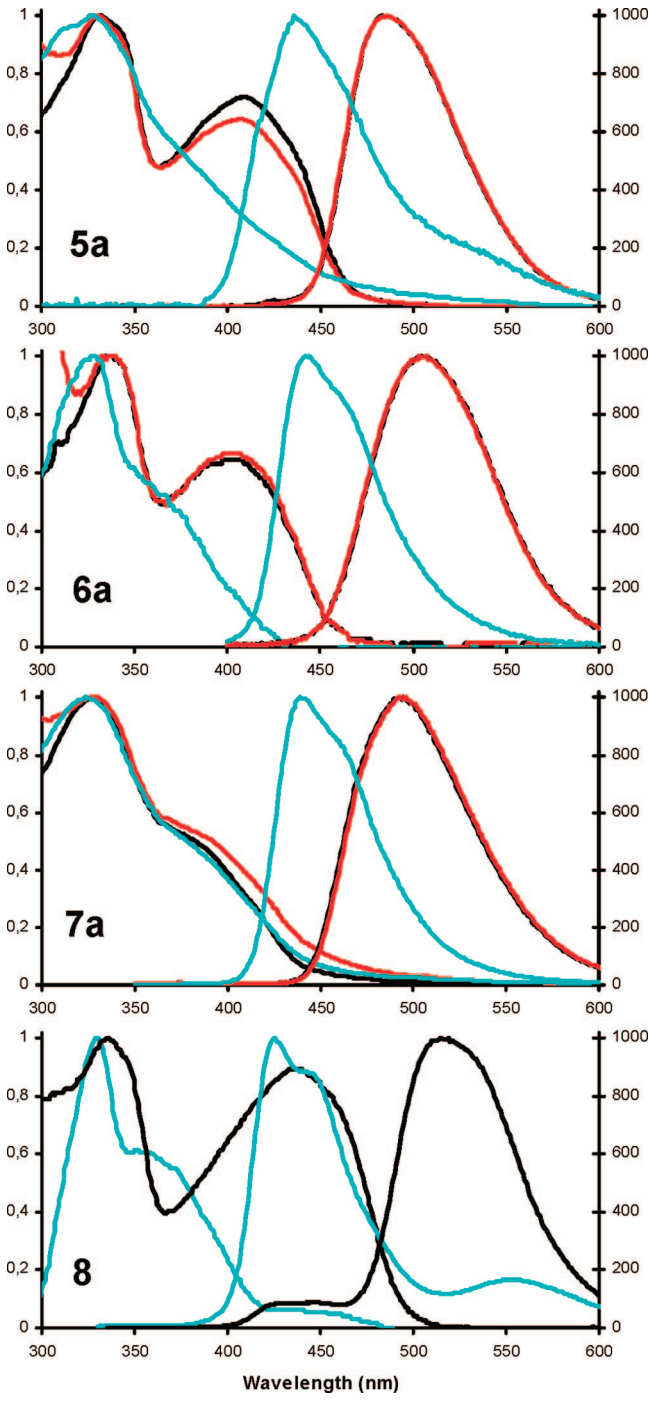

Figure 1. Normalized absorption and emission spectra of **5a**, **6a**, **7a**, and **8** in dichloromethane (black traces) and after addition of 50 μL (0.66 mmol; 66 mmol·L^{-1}; 6.6 × 10^4 equiv) of trifluoroacetic acid (TFA, blue traces **5a**, **6a**, **7a**, **8**) or 50 μL (0.36 mmol, 36 mmol·L^{-1}; 3.6 × 10^4 equiv) of triethylamine (red traces **5a**, **6a**, **7a**). For **5a** and **6a**, the triethylamine and dichloromethane traces in emission are perfectly overlapping, so that only either the red or the black traces are visible. The spectra are taken at a concentration of 1 μmol·L^{-1} XF.

water are different from those of **5a** and **6a** in dichloromethane. The charge transfer band (CT band) is significantly reduced; the UV–vis spectrum of **7a** in water is similar to that of **7b** in chloroform. A qualitative explanation assumes the repulsion of like (negative) charges, leading to deplanarization of the amine groups in **5b** and **6b** with respect to the π-system of the distyrylbenzene. Enhanced intramolecular hydrogen bonding between the carboxylic acids, the carboxylates, and the anilines

Table 1. Absorption and Emission Data of XFs **5a**–**7a** and **8** in CH_2Cl_2 1 μmol·L^{-1} Concentration of XF in Neutral, Acid, and Basic Conditions

CH_2Cl_2	5a	6a	7a	8
absorption (nm)	333, 411	338, 405	328	336, 440
emission (nm)	486	506	494	518
TFA added absorption (nm)	330	329	326	331
TFA added emission (nm)	439	443	442	427, 558
NEt_3 added absorption (nm)	332, 409	338, 404	329	N/A
NEt_3 added emission (nm)	486	505	495	N/A

leads to a hydrogen-bonded network, preferring a conformation in which the free electron pairs of the aniline nitrogens of **5b** and **6b** are twisted out of the plane of the distyrylbenzene unit. In the emission spectra, this effect is less pronounced; the emission spectra of **5b** and **6b** in dilute solution are red-shifted as compared to that of **8**. However, in the case of **7b**, the emission is centered around 450 nm, suggesting that the combination of both the steric hindrance and electrostatic repulsion decouples the amino groups electronically from the distyrylbenzene skeleton. The absorption spectra of **5b** and **7b** are concentration-independent, while the absorption spectrum of **6b** changes with concentration (Figure 4). At low concentration (light green, 5 μmol·L^{-1}), the CT band is not visible, while at 100 μmol·L^{-1}, the CT band is prominent at 393 nm; the concentration-dependent change in the absorption spectra of **6b** suggests a ground-state interaction of two or more molecules of **6b**, acting by either mechanical/electrostatic agglomeration-induced planarization or the formation of electronic aggregates.

The concentration effects in emission are more pronounced. For **5b**, no concentration-dependent change in emission is recorded, but both **6b** and **7b** experience a significant shift in emission when increasing their concentration from 1 to 100 μmol·L^{-1}. While the emission of **6b** red shifts from 458 to 537 nm, that of **7b** changes from 439 to 524 nm. This concentration dependence suggests excimeric species in **6b** and **7b** but not in **5b**. Both **6b** and **7b** show blue-shifted emission bands at low concentrations that in **8** would be indicative for metal binding, protonation, or twisting around the aniline nitrogen. As we work in buffered solution at pH 7.0, protonation of the aniline nitrogen is rejected. To exclude self-absorption effects in the case of **6b**, we performed fluorescence measurements in a triangular cuvette, and the obtained spectra (see Supporting Information) are identical to those we recorded for **6b** in regular cuvettes.

The fluorescence quantum yields of **5b**−**7b** in water are low at physiological pH (Table 1); the XF **7b** shows the highest quantum yield (Φ = 4.4%) in water. While **6b** is almost

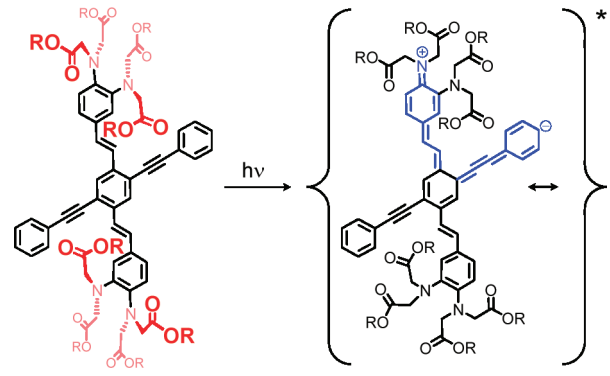

Figure 2. Proposed excited state planarization of **7**.

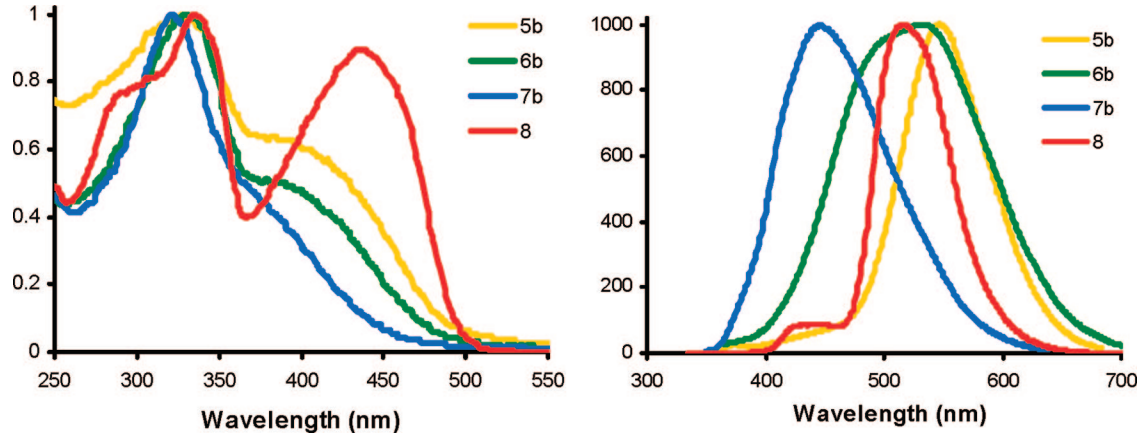

Figure 3. Overlaid normalized absorption and emission spectra of **5b**, **6b**, and **7b** in phosphate buffered (100 mmol·L^{-1}) aqueous solution and **8** in dichloromethane as 10 μmol·L^{-1} solutions.

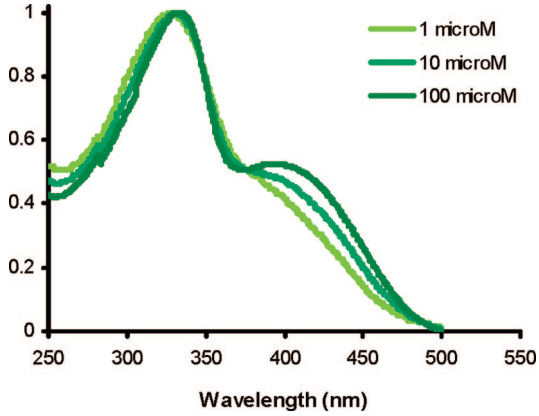

Figure 4. Absorption spectra of **6b** at concentrations of 1, 10, and 100 μmol·L^{-1} in phosphate buffered (100 mmol·L^{-1}) aqueous solution.

nonfluorescent, **5b** displays a Φ of 0.8%. While these quantum yields are somewhat dissappointing, they are not unusual for organic chromophores in aqueous solution. Water as a highly polar solvent stabilizes excited zwitterionic CT states, which will then efficiently deactivate. We investigated the emission profiles of **5b**−**7b** with respect to different excitation wavelengths. While both **5b** and **7b** show only minute changes in their emission spectra, the XF **6b** experiences significant spectral changes modulation upon modulating the excitation wavelength; indeed, there is a significant wavelength dependency of the excitation spectra (see Figures 5 and 6, right part).

We explain this behavior as a consequence of coplanarization of the amine groups in XF **6b**. If we irradiate at low wavelengths (high energy), the nonplanarized molecules are preferentially excited and emission from nonplanarized excited states is observed. If irradiated at lower frequencies, only planarized molecules are excited and therefore preferred emission from planar XFs **6b** is observed as a result. We presume that, in **6b**, in the ground state, there is a thermal distribution of planarized and nonplanarized forms of the XFs, leading to the wavelength-dependent emission spectra. In **5b**, **8**, and **7b**, on the other hand, there is either the mostly planarized form (**5b**, **8**) or the predominantly twisted form (**7b**) present. The propensitiy for the twisting of the aniline unit is a function of the increasing steric hindrance and the electrostatic repulsion of the negative charges when going from **5b** to **7b**. The APTRA-type XF **6b** seems intermittent in its ability to planarize. However, the emission spectra taken from very dilute solutions suggest that isolated **6b** is preferentially in its twisted form as it is blue emissive. We examined the ionic strength dependency of the emissive properties of **6b** and **7b** by addition of a large excess of $KClO_4$ and did not see any effect on fluorescence wavelength or intensity. Metal sensing with ligand systems such as **6b** or **7b** will probably not work by the same mechanism that we have found to be operative for **8**, but instead possibly by breakup of aggregates (vide infra).

Investigation of the pH Dependency of Absorption and Emission in 5b–7b. As **5b–7b** have acidic and basic functionalities, their pH-dependent photophysical properties were of great interest. Figure 7 displays absorption and emission spectra of **5b–7b** under neutral (pH 7.0), basic (pH 14), and acidic (pH 1.6) conditions. The spectra are taken at a 5 μmol·L^{-1} concentration of the respective XF, with exception of the black

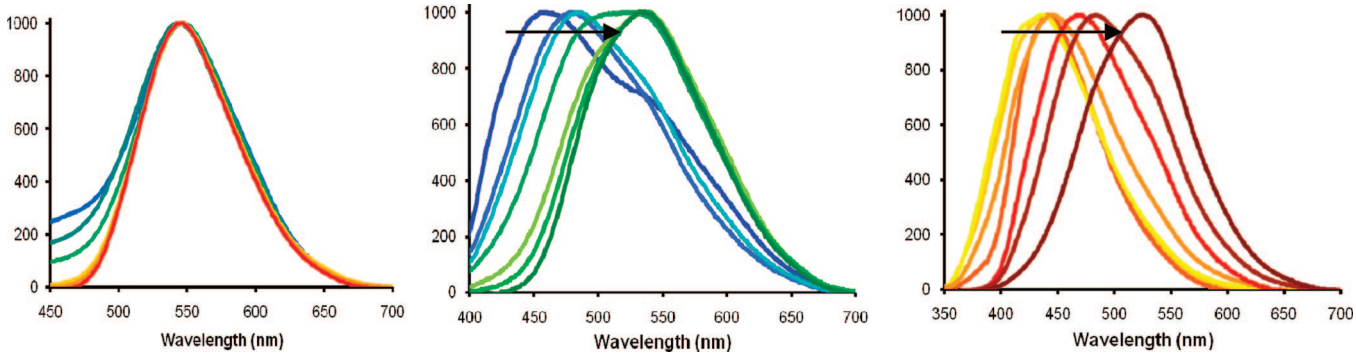

Figure 5. Emission of **5b** (left), **6b** (middle), and **7b** (right) in phosphate buffer (100 mmol·L^{-1}) at 1, 2, 5, 10, 25, 50, and 100 μmol·L^{-1} concentrations. The arrow displays increasing concentration of the respective cruciform.

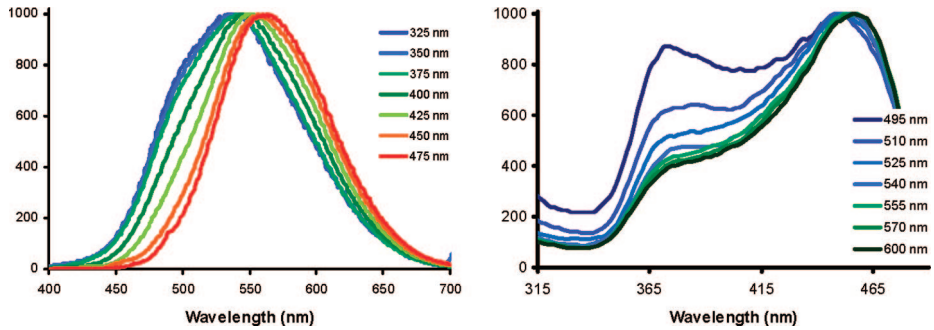

Figure 6. Emission spectra of **6b** under excitation at 325, 350, 375, 400, 425, 450, and 475 nm at 50 μmol·L^{-1} concentration in phosphate buffered (100 mmol·L^{-1}) aqueous solution. Scattering peaks and peaks due to lamp profile are subtracted out (left). Normalized excitation spectra of **6b** at different wavelengths. At an increasing excitation wavelength, the feature at 465 nm increases (right).

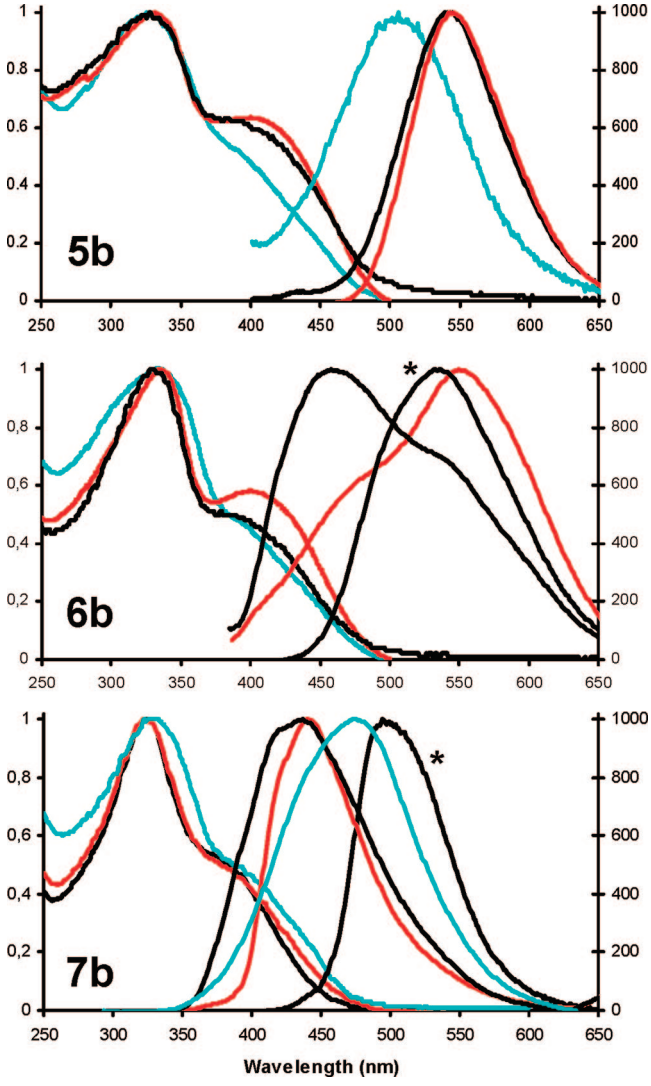

Figure 7. Normalized absorption and emission spectra of **5b** (top), **6b** (middle), and **7b** (bottom) under neutral (black, pH 7.0), acidic (blue, pH 1.6), and basic (red, pH 14) conditions. The concentration of the XFs was 5 μmol·L^{-1}. For the starred black lines, the XF concentration was 100 μmol·L^{-1}.

traces marked with a red asterisk. These spectra were taken at 100 μmol·L^{-1} concentration of XF for comparison. Upon addition of acid, the fluorescence of **5b** is greatly reduced but blue-shifted to 506 nm. We attribute the blue shift to the protonation of the aniline nitrogen, leading to a significant stabilization of the HOMO. At a pH of 1.6, however, not only the aniline units but also the carboxylic acid units are protonated. In the structurally similar phenyl imidobisacetic acid, the pK_a values are 6.4, 4.6, 3.5, and 3.0.[31] In absorption, the expected blue shift and a loss of the CT band is observed, similar as reported for the model compound **8**. In the case of **6b**, protonation leads to quenching of the fluorescence of the XF. In absorption, the pH-dependent changes are subtle. Blue shifts and intensity reductions of the CT bands of XFs are recorded.

In **7b**, the absorption is almost pH-independent, but the emission red shifts upon protonation from 437 to 476 nm, while at pH 14, the emissive maximum is at 440 nm, that is, blue, suggesting deplanarization of the aniline lone pairs. The red shift in emission at pH 1.6 might be due to partial planarization in the excited state, enabled by the removal of the electrostatic repulsion between the formerly negatively charged acetate (now acetic acid) groups.

This hypothesis is borne out by the significant red shift of the emission spectra of both **6b** and **7b** upon a pH increase. This shift is concentration-independent, which excludes excimer formation or other intermolecular mechanisms for the red shift in the emission of **6b** and **7b**. Again, **5b** as a sterically less encumbered species does not show significant emission shifts upon going from neutral buffered into basic solution.

Metal-Responsive Properties of 5b–7b in Aqueous Buffered Solution. The most enticing aspect of water-soluble chromophores and fluorophores is their interaction with metal cations under physiological conditions. Questions of the quantity and distribution of pools of free transition metal cations such as zinc or copper in cells are connected with neurophysiological function and disease states of the central nervous system and the brain. Zinc cations are suspected to play a role in the formation of plaques; enhanced levels of Zn^{2+} ions is found in the brains of deceased Alzheimer patients.[15,32]

With the water-soluble XFs **5b**−**7b** in hand and armed with the knowledge gained from the investigation of the model XF **8** and its interaction with metal cations,[16b,d] we exposed the XFs **5b**−**7b** to different metal salts (0.4 mmol·L^{-1} metal salt, XF either 5 or 50 μmol·L^{-1}). We performed these experiments in PIPES buffer (100 mmol·L^{-1}, Figure 8). The XF **5b** is quenched upon addition of Hg^{2+}, Cu^{2+}, and Zn^{2+}, while for **6b**, its color changes upon exposure to Zn^{2+}. Using a 50 μmol·L^{-1} solution of XF gives a significantly enhanced emissive response. For **6b**, Mg^{2+} and Ca^{2+} cations respond

(31) Sanchiz, J.; Dominguez, S.; Mederos, A.; Brito, F.; Arrieta, J. M. *Inorg. Chem.* **1997**, *36*, 4108–4114.
(32) Burdette, S. C.; Lippard, S. J. *Coord. Chem. Rev.* **2001**, *216*, 333–361.

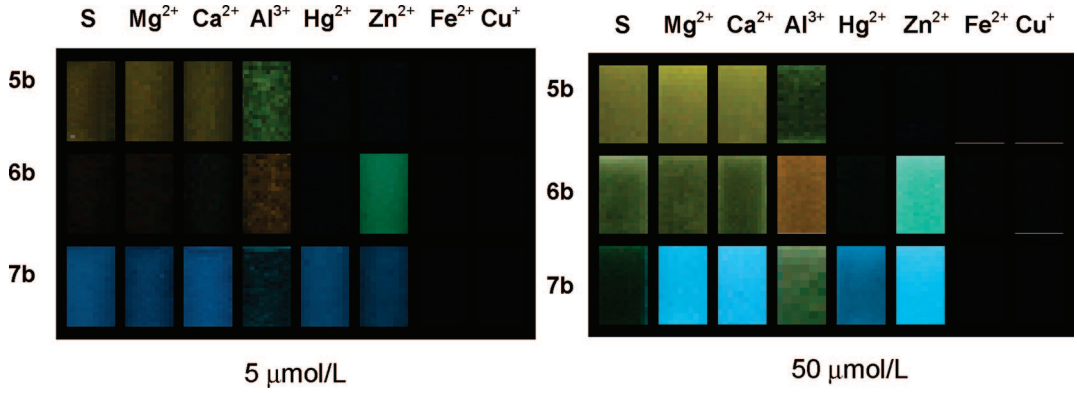

Figure 8. Qualitative results of the sensing of metal cations (0.4 mmol·L^{-1}) by the three XFs **5b**–**7b** in PIPES solution.

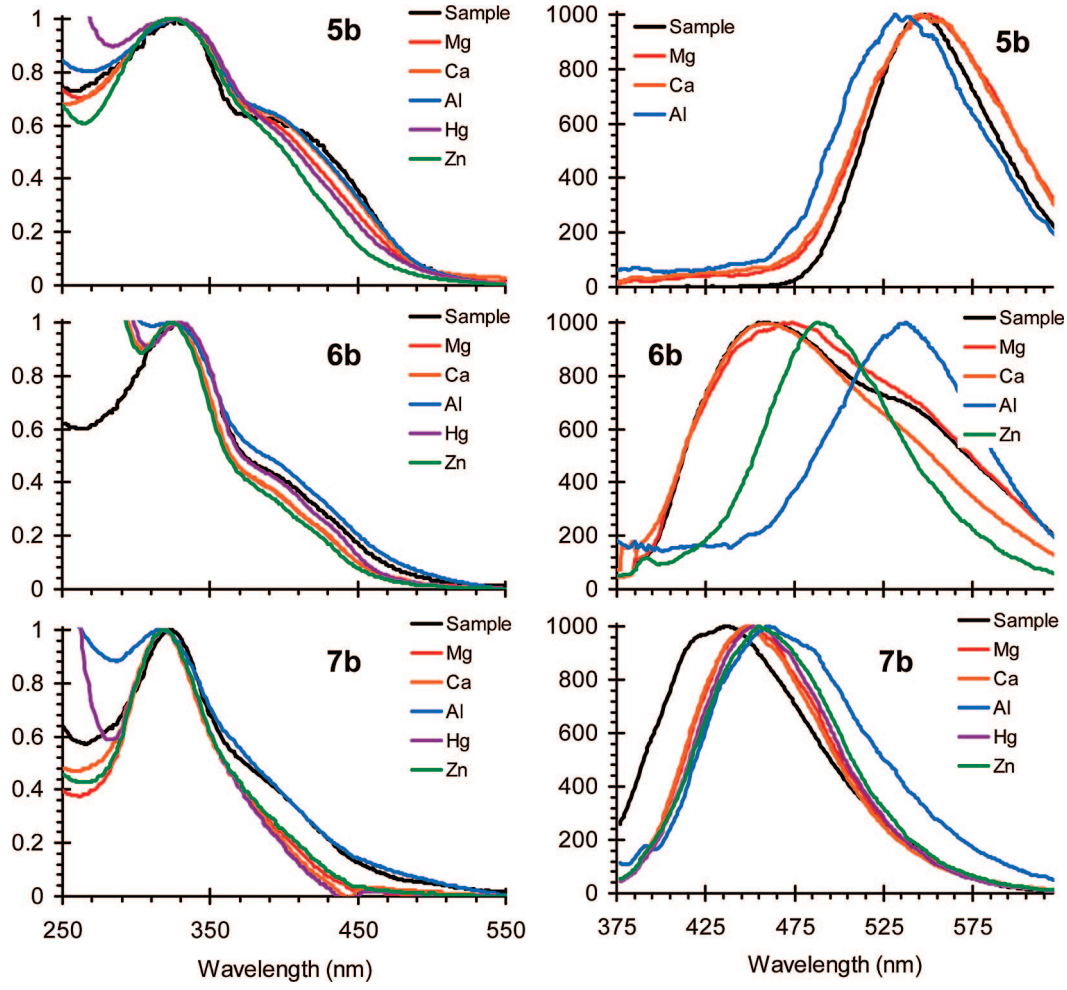

Figure 9. Interaction of metal cations (Mg^{2+}, Ca^{2+}, Al^{3+}, Hg^{2+}, Zn^{2+}; 0.4 mmol·L^{-1}) with the three XFs **5b**–**7b** at 5 μmol·L^{-1} concentration in aqueous PIPES solution at pH 7.2. Normalized absorption spectra are displayed on the left, and normalized emission spectra are displayed on the right.

weakly, but Hg^{2+} and Cu^{2+} effectively quench the fluorescence of **6b**. Zinc ions induce a significant color shift, from orange to blue, while Al^{3+} increases the fluorescence intensity. The XF **7b** (50 μmol·L^{-1}) experiences an increase in fluorescence for the addition of Mg^{2+}, Ca^{2+}, Hg^{2+}, and Zn^{2+}, while Al^{2+}, Fe^{3+}, and Cu^{2+} do not lead to a change in the emission at all. If we perform the experiments in a solution 5 μmol·L^{-1} in XF, only Fe^{3+} and Cu^{2+} quench the fluorescence of **7b**, other metal cations do not have an effect on the fluorescence.

Figures 9 and 10 display the accompanying spectra to the pictorial description in Figure 8. Important points are gleaned from Figures 8−10 and Tables 2 and 3, where the emissive lifetimes of XFs **5b**−**7b** at different concentrations and in the presence and the absence of zinc ions are on display. The three seemingly similar compounds **5b**–**7b** feature metalloreactivities that are dependent upon their concentration, particularly in the case of **6b** and **7b**. At 5 μmol concentrations, XF **6b** does not show any metal reactivity; however, at a concentration of 50 μmol·L^{-1}, the metalloreactivity, particularly to zinc, is noticeable. A shift from yellow-orange to blue occurs in the fluorescence. In solutions of **6b** at 50 μmol·L^{-1} concentration, excimers persist, leading to a red-shifted, excimeric emission

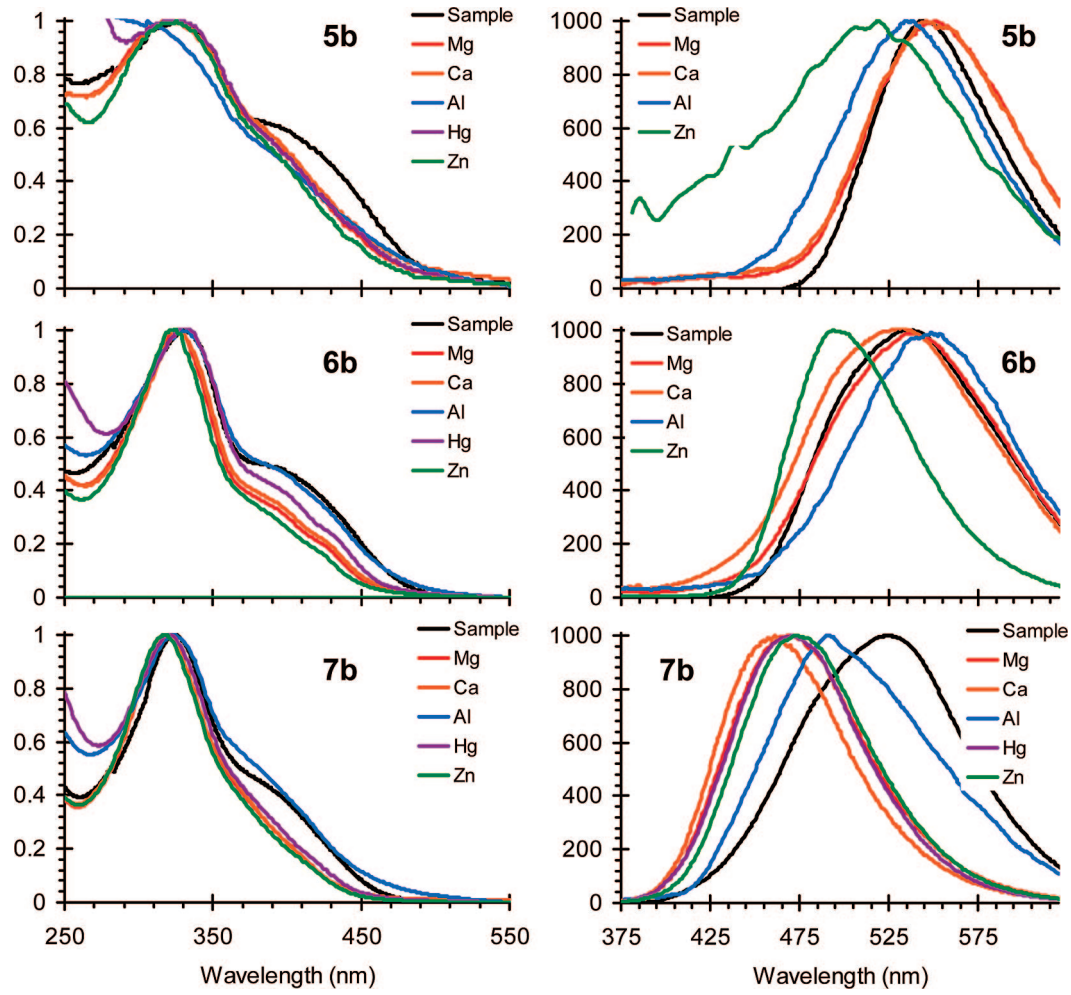

Figure 10. Interaction of metal cations (Mg^{2+}, Ca^{2+}, Al^{3+}, Hg^{2+}, Zn^{2+}; 0.4 mmol·L^{-1}) with the three XFs **5b**–**7b** at 50 μmol·L^{-1} concentration in aqueous PIPES solution at pH 7.2. Normalized absorption spectra are displayed on the left, and normalized emission spectra are displayed on the right.

Table 2. Absorption and Emission Data of XFs **5b**−**7b** in Water (Phosphate Buffer, 100 mmol·L^{-1}, pH = 7.0) 10 μmol·L^{-1} Concentration of XF

H_2O pH 7.0	**5b**	**6b**	**7b**
absorption (nm)	328	329	322
emission (nm)	546	531	446
Stokes shift (nm)	12172	11563	8634
Φ (%)	0.8	<0.5	4.4
ε (l mol^{-1} cm^{-1})	53500	48000	54000

(Table 2) complemented by a decrease of the emissive lifetime from 1.5 to 0.8 ns. Upon addition of zinc cations, but not upon the addition of Ca^{2+} or Mg^{2+}, the blue fluorescence of the monomeric species is restored and the emissive lifetime is increased to 1.6 ns, suggesting either the suppression or the breakup of excimeric species of **6b** by zincation.

We see a similar effect in **7b**, which is weakly fluorescent at a 50 μmol concentration. The addition of mercury, magnesium, calcium, or zinc cations leads to a strong increase in fluorescence intensity but without a large shift in emission wavelengths. Investigation of the emissive lifetimes of **7b** in dilute (Table 2, τ = 2.4 ns) and concentrated (τ = 1.2 ns) solution before and after the addition of zinc ions to a concentrated solution of **7b** (τ = 2.4 ns) suggests the formation and disruption/suppression of excimers as the mechanism of metalloresponsivity of **7b**; however, the "excimers" formed from **7b** are self-quenching and almost nonfluorescent instead of red-shifted.

Table 3. Emissive Liftime Data of Cruciforms **5b**−**7b** (pH 7.0 Phosphate Buffer, 100 mmol·L^{-1})

XF	concentration (μM)	metal	λ_{max} emission (nm)	τ (ns)
7b	2		450	2.4
	5		460	2.6
	50		531	1.2
	100		531	1.4
	5	Zn^{2+}	455	2.7
	50	Zn^{2+}	455	2.5
6b	2		446	1.5
	5		446	1.4
	50		519	0.8
	100		530	0.7
	5	Zn^{2+}	471	1.8
	50	Zn^{2+}	471	1.6
5b	2		546	0.8
	5		546	0.8
	50		546	0.8
	100		546	0.8
	5	Zn^{2+}	535	0.9
	50	Zn^{2+}	535	0.9

In the case of **5b**, excimers do not form, and the lifetime does not change, even if we inspect aqueous solutions that are 100 μmol in concentration. The metalloresponsivity of **5b** disappoints. The addition of Mg^{2+}, Ca^{2+}, Al^{3+}, or Fe^{3+} cations does not change the fluorescence of **5b** at all, while mercury, zinc, and copper simply quench the fluorescence of **5b**. When

investigating **5b** in aqueous buffer, Zn^{2+} and Hg^{2+} change the absorption of **5b**, leading to a modest weakening of the CT band.

The classic explanation of the change in the absorption spectrum and quenching in the emission spectrum would invoke partial excited state decomplexation,[3,33,34] resulting in species where the metal cation is only loosely bound to the fluorophore but assists in vibrational or otherwise radiationless deactivation of the excited state. However, the complexation of the weakly binding XF **8** with zinc or magnesium salts in dichloromethane results in a strong blue shift of the emission, suggesting that, by analogy, excited state decomplexation is not a probable mechanism for the quenching of **5b**. We hypothesize that the binding of **5b** to Zn^{2+} or Hg^{2+} ions in aqueous buffered solution will stabilize the excited state. It is coupled to an overtone vibration of water molecules coordinated to either Zn^{2+} or Hg^{2+} ions and therefore will promote radiationless deactivation of the fluorescence. If we examine the emission of **5b**−**7b** in D_2O as opposed to H_2O, the fluorescence intensity increases by a factor of 2–4, regardless of the presence or absence of metal cations. While this observation suggests some vibrational coupling of the excited states of **5b**−**7b** to suitable overtone vibrations of water, the fluorescence quantum yields in D_2O are still not very high, suggesting that other factors also play a significant role; however, ionic strength (vide supra) does not seem to be one them.

Conclusions

The water-soluble XFs **5b**−**7b** were synthesized by a combination of Horner reaction, Sonogashira coupling, and subsequent saponification. The photophysical properties of **5b**−**7b** and their metalloreactivity were examined and compared to that of the model compound **8**. It is noted that the metalloresponsive properties of **5b**−**7b** in aqueous buffered solution are fundamentally different from those of the model system **8** possessing the same fluorophore. While the low fluorescence quantum yields for **5b**−**7b** in water were not unexpected, the blue-shifted emission of **6b** and **7b** in the absence of metal ions in water was surprising at first but is explained by a combination of electrostatic repulsion of the negatively charged carboxylate groups and the significant steric crowding. In the case of **6b**, an attractive zinc-specific response was found, which was based upon the breakup of excimeric species rather than upon the specific binding of the zinc cations to the lone pair of the aniline nitrogen in the APTRA motif of **6b**. While APTRA and similar motifs are popular and successful in the detection of metal cations in cellular environs and compartments, they may act not only by the normally proposed coordination mechanism but also by breakup of aggregates and even, as suggested in the literature, by interaction of intact dye nanoparticles with metal cations after endocytosis into the cell.[4] We note that the investigation of organo-soluble model compounds such as **8** is invaluable to understand the innate properties of a metalloresponsive species. The attachment of charged appendages and water as solvent fundamentally changes the fluorescent responses of XFs but in difficult to predict ways. Without the careful investigation of **8**, the interpretation of the results obtained for **5b**−**7b** would have been difficult and perhaps misleading.

Acknowledgment. We thank the Department of Energy (DE-FG02-04ER46141) for financial support, Prof. Laren Tolbert and Prof. Christoph Fahrni for helpful discussions, and Prof. Rob Dickson for the use of the CAROM lifetime spectroscopy setup. J.T. thanks Junta de Comunidades de Castilla La Mancha (Fondo Social Europeo FSE 2007-2013) for his post-doctoral grant.

Supporting Information Available: Experimental details are provided for the synthesis of XFs **5**–**7**, as well as details for the photophysical experiments. This material is available free of charge via the Internet at http://pubs.acs.org.

JA800232F

(33) (a) Fery-Forgues, S.; Le Bris, M.-T.; Guette, J.-P.; Valeur, B. *J. Phys. Chem.* **1988**, *92*, 6233–6237. (b) Bourson, J.; Valeur, B. *J. Phys. Chem.* **1989**, *93*, 3871–3876. (c) Rurack, K.; Rettig, W.; Resch-Genger, U. *Chem. Commun.* **2000**, 407–408. (d) Bricks, J. L.; Slominskii, J. L.; Kudinova, M.; Tolmachev, A. I.; Rurack, K.; Resch-Genger, U.; Rettig, W. *J. Photochem. Photobiol. A* **2000**, *132*, 193–208.

(34) (a) Das, S.; Thomas, K. G.; Thomas, K. J.; Kamat, P. V.; George, M. V. *J. Phys. Chem.* **1994**, *98*, 9291–9296. (b) Marcotte, N.; Fery-Forgues, S.; LavabreD.; Marguet, S.; Pivovarenko, V. G. *J. Phys. Chem. A* **1999**, *103*, 3163–3170. (c) Marcotte, N.; Plaza, P.; Lavabre, D.; Fery-Forgues, S.; Martin, M. M. *J. Phys. Chem. A* **2003**, *107*, 2394–2402.